LBL-21144
UC-95c

Lawrence Berkeley Laboratory
UNIVERSITY OF CALIFORNIA

APPLIED SCIENCE DIVISION

RECEIVED
LAWRENCE
BERKELEY LABORATORY

APR 22 1988

LIBRARY AND
DOCUMENTS SECTION

The Exponential Scheme for Computation of Natural Convection Flow in Enclosures

L.C. Huang

January 1988

For Reference

Not to be taken from this room

APPLIED SCIENCE
DIVISION

Prepared for the U.S. Department of Energy under Contract DE-AC03-76SF00098

LBL-21144

DISCLAIMER

This document was prepared as an account of work sponsored by the United States Government. While this document is believed to contain correct information, neither the United States Government nor any agency thereof, nor the Regents of the University of California, nor any of their employees, makes any warranty, express or implied, or assumes any legal responsibility for the accuracy, completeness, or usefulness of any information, apparatus, product, or process disclosed, or represents that its use would not infringe privately owned rights. Reference herein to any specific commercial product, process, or service by its trade name, trademark, manufacturer, or otherwise, does not necessarily constitute or imply its endorsement, recommendation, or favoring by the United States Government or any agency thereof, or the Regents of the University of California. The views and opinions of authors expressed herein do not necessarily state or reflect those of the United States Government or any agency thereof or the Regents of the University of California.

THE EXPONENTIAL SCHEME FOR COMPUTATION OF NATURAL CONVECTION FLOW IN ENCLOSURES

Lan Chieh Huang*

Simulation Research Group
Lawrence Berkeley Laboratory
University of California
Berkeley, California

Abstract

In this paper the exponential scheme for multi-dimensional unsteady problems is discussed; a basis for approximation of solution is given and a boundary exponential scheme is derived. It is applied to the computation of natural convection in a square cavity with moderate size uniform grid for future calculation of air flow in enclosures and heat flux at walls in building energy analysis. The numerical method for the Boussinesq equations is based on the Marker and Cell (MAC) method and is put into conservation form via the Spalding-Patankar flux. The latter method is also discussed. Preliminary numerical tests show that the method is promising.

January 1988

This work was supported by the Assistant Secretary for Conservation and Renewable Energy, Office of Building and Community Systems, Building Systems Division of the U. S. Department of Energy under Contract No. DE-AC03-76SF00098.

*Permanent address: Computing Department, Chinese Academy of Sciences, Beijing, P.R. China.

Introduction

In recent years, numerical solution of natural convection flow in enclosures has gained much interest in the computational fluid dynamics community. Its applications include such problems as reactor insulation, cooling of radioactive waste containers, solar energy collection, ventilation of rooms, and energy conservation in buildings [1] which is the main interest of the present work. The governing equations are the Boussinesq approximation equations, which are very similar to the incompressible Navier-Stokes equations. We will be concerned with solution in the primitive variable form, so that extension to the three-dimensional case will be straightforward.

For large scale phenomena, many finite difference schemes on uniform grids can be used, such as some of the ones quoted in the comparison exercise of DeVahl Davis and Jones [2]. But for resolution of boundary layers and other small scale phenomena, the standard methods have proved to be too expensive in terms of computer time, especially for high Rayleigh numbers, which correspond to high Reynolds numbers and very thin boundary layers. The goal of the present work is to find a method which will work on moderate size uniform grids and which will give reasonably accurate heat fluxes at the walls.

The dominant feature in the boundary layer at the walls in buildings is that the solution has large gradients. We consider its approximation by exponential functions and test the exponential scheme. In general, this scheme is understood only in the one-dimensional steady-state case. In this paper, a basis for approximation of the solution is given for the multi-dimensional unsteady exponential scheme, along with a boundary nonuniform grid exponential scheme. The author hopes that this will lead to better understanding and more selective use of the scheme.

The Spalding-Patankar scheme [3] will also be discussed. Its one-dimensional hybrid version happens to be accurate for high cell Reynolds number calculation and its exponential version turns out to be the same as the exponential schemes for uniform grids. But for nonuniform grids, this scheme is, in general, not consistent with the original partial differential equation.

The solution of the Boussinesq equations is based on the MAC method of Harlow and Welch [4] in that the staggered mesh is used and the Poisson equation for pressure enforcing the divergence-free constraint is obtained from the momentum equations. The equivalence between the partial differential equations is retained in difference form; with this equivalence, computation can proceed without a devastating accumulation of errors. The exponential scheme is put into conservation form via the Spalding-Patankar flux and is adapted to the non-linear system of partial differential equations. The conservation form facilitates computation in general and the equivalence mentioned above. Only numerical results for the standard model test problem of natural convection in a rectangular cavity with aspect ratio 1, Prandtl number 0.71, Rayleigh number 10^6 and 10^7 are presented in this paper. From these preliminary results, we see that with one

mesh point in the boundary layer, the accuracy of the average Nusselt number at steady-state suffices for the present problem.

1. The Boussinesq Equations and the Model Problem

The Boussinesq equations governing natural convection flow are obtained from the Navier-Stokes equations under the assumption that

$$\rho = \rho_o + \Delta\rho \qquad \Delta\rho/\rho_o << 1$$

$$T = T_o + \Delta T \qquad \Delta T/T_o << 1$$

where ρ_o and T_o are the mean density and temperature, respectively. Let us scale pressure and temperature as

$$\phi = p - p_s \qquad \theta = \frac{T - T_o}{\delta T}$$

where p_s relates to a field with zero velocity, i.e. $\nabla p_s = \rho_o \vec{g}$, and where δT is some characteristic temperature difference.

Let us choose length L as the characteristic length, ρ_o the characteristic density, $V_o = \mu/\rho_o L$ (μ, the fluid viscosity) the characteristic velocity, L/V_o the characteristic time, and $\rho_o V_o^2$ the characteristic pressure. Then the non-dimensional form for the two-dimensional case is

$$\frac{\partial u}{\partial x} + \frac{\partial v}{\partial y} = 0 \quad or \quad D = 0 \tag{1.1}$$

$$\frac{\partial u}{\partial t} + u\frac{\partial u}{\partial x} + v\frac{\partial u}{\partial y} + \frac{\partial \phi}{\partial x} = \frac{\partial^2 u}{\partial x^2} + \frac{\partial^2 u}{\partial y^2} \tag{1.2}$$

$$\frac{\partial v}{\partial t} + u\frac{\partial v}{\partial x} + v\frac{\partial v}{\partial y} + \frac{\partial \phi}{\partial y} = \frac{\partial^2 v}{\partial x^2} + \frac{\partial^2 v}{\partial y^2} + Gr\ \theta \tag{1.3}$$

$$\frac{\partial \theta}{\partial t} + u\frac{\partial \theta}{\partial x} + v\frac{\partial \theta}{\partial y} = \frac{1}{Pr}\left(\frac{\partial^2 \theta}{\partial x^2} + \frac{\partial^2 \theta}{\partial y^2}\right) \tag{1.4}$$

where

$$Gr = \frac{\rho_o^2\, \beta\, g\, L^3\, \delta T}{\mu^2}$$

is the Grashof number (β, the thermal expansion coefficient of the fluid) and where

$$Pr = \frac{\mu\, c_p}{\kappa}$$

is the Prandtl number (c_p, the specific heat at constant pressure; κ the coefficient of thermal conductivity). The product of these two numbers is defined as the Rayleigh number, i.e.

$$Ra = Gr \cdot Pr$$

Momentum equations (1.2) and (1.3) and energy equation (1.4) are evolutionary, but mass equation (1.1) is not; it can be considered as a constraint to the system. The model problem which we will consider is the buoyancy driven flow in a rectangular cavity of width L and height H, with temperature T_h on the left vertical wall, and T_c on the right vertical wall, and with an adiabatic condition on the top and bottom walls. The no-slip condition for velocity applies on all the four walls. Taking L as the characteristic length and $\delta T = T_h - T_c$, the non-dimensional form of the boundary conditions is

$$\theta(0,y) = \theta_h \qquad 0 \leq y \leq H/L \tag{1.5}$$

$$\theta(1,y) = \theta_c \qquad 0 \leq y \leq H/L$$

$$\frac{\partial\theta}{\partial y}(x,0) = \frac{\partial\theta}{\partial y}(x,H/L) = 0 \qquad 0 \leq x \leq 1 \tag{1.6}$$

$$u(x,y) = v(x,y) = 0 \qquad x=0 \ \ or \ \ 1 \tag{1.7}$$

$$y=0 \ \ or \ \ H/L$$

as indicated in figure 1.

Before attempting the numerical solution of the Boussinesq equations, we will discuss some of the difficulties which may come up in the computation of this type of problem with simpler linear scalar equations.

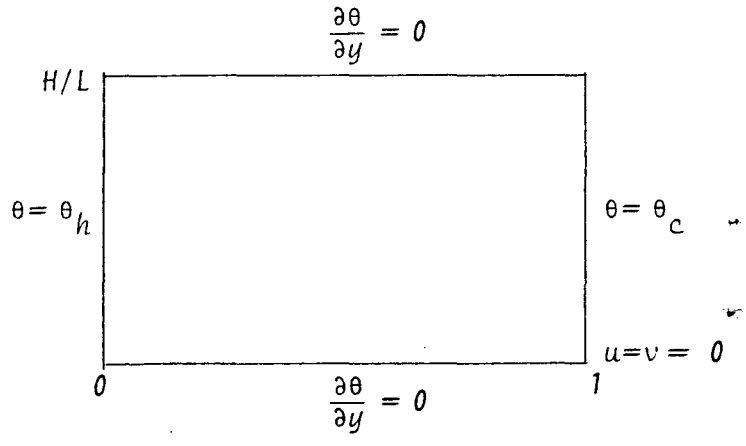

Figure 1

2. Properties of Some Finite Difference Schemes

Let us consider the one dimensional steady-state convection-diffusion equation

$$a \frac{df}{dx} - \alpha \frac{d^2 f}{dx^2} = 0 \ , \ 0 \leq x \leq l \tag{2.1}$$

where a and α are constants >0, with boundary conditions

$$f(0) = 0 \ , \ f(l) = 1 \tag{2.2}$$

This problem has the exact solution

$$f(x) = C_1 + C_2 \, e^{ax/\alpha} \tag{2.3}$$

where

$$C_1 = \frac{f(0)\, e^L - f(l)}{e^L - 1}$$

$$C_2 = \frac{f(l) - f(0)}{e^L - 1} \tag{2.4}$$

and $L = al/\alpha$. We know that for large $Re = a/\alpha$, the solution has large gradient near the right boundary (see fig. 2). Numerical solution of this type of problem poses certain difficulties and some of these difficulties will be discussed with a few standard finite difference schemes in the following.

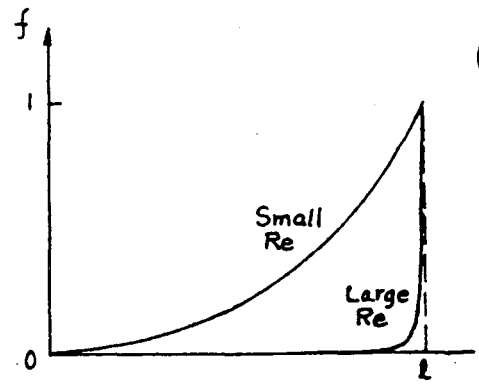

Figure 2

The centered difference scheme (C):

$$a \frac{f_{j+1} - f_{j-1}}{2\Delta x} - \alpha \frac{f_{j+1} - 2f_j + f_{j-1}}{\Delta x^2} = 0 \tag{2.5}$$

where $1 \leq j \leq J-1$, $J\Delta x = l$. It is of formal second order accuracy; i.e., for fixed α and sufficiently small Δx, the truncation error is $O(\Delta x^2)$.
But for cell Reynolds number

$$R = \frac{a \ \Delta x}{\alpha} > 2$$

the numerical solution will usually have oscillations. This can be seen from the exact solution of (2.5). We try $f_j = \lambda^j$ and obtain a quadratic equation in λ with roots

$$\lambda_1 = 1 \quad , \quad \lambda_2 = \frac{2+R}{2-R} \tag{2.6}$$

The general solution of (2.5) is $f_j = C_1 + C_2 \lambda_2^j$, where C_1 and C_2 are determined by the boundary conditions. For $R > 2$, λ_2 is negative and λ_2^j will take on values with opposite signs as j increases (or decreases), hence f_j will oscillate, unless for certain boundary conditions $C_2 = 0$.

The first order upwind difference scheme ($U1$):

$$a \frac{f_j - f_{j-1}}{\Delta x} - \alpha \frac{f_{j+1} - 2f_j + f_{j-1}}{\Delta x^2} = 0 \tag{2.7}$$

If we solve for the exact solution as above, we will obtain the corresponding roots

$$\lambda_1 = 1 \quad , \quad \lambda_2 = 1 + R \tag{2.8}$$

which are positive for all R; hence there will be no oscillation. However, it is only of formal first order accuracy.

It is to be expected that some second order upwind difference scheme be considered as an improvement of the first order ones. We mention two here: the first one [5] is well known, the Leonard upwind difference scheme (L):

$$a \frac{f_{j+½} - f_{j-½}}{\Delta x} - \alpha \frac{f_{j+1} - 2f_j + f_{j-1}}{\Delta x^2} = 0 \tag{2.9}$$

$$f_{j+½} = \frac{1}{2}(f_{j+1} + f_j) - \frac{1}{8}(f_{j+1} - 2f_j + f_{j-1})$$

It is of formal second order accuracy, but one of the roots λ_i will be negative if

$$R > \frac{8}{3}$$

Hence there will still be oscillation.

If we use the most common second order one-sided difference, we get the formal second order upwind difference scheme ($U2$):

$$a \frac{3f_j - 4f_{j-1} + f_{j-2}}{2\Delta x} - \alpha \frac{f_{j+1} - 2f_j + f_{j-1}}{\Delta x^2} = 0 \tag{2.10}$$

Now, all roots λ_i are positive for all R, hence there will be no oscillation. This scheme works well for some purposes though its realization may be troublesome.

We look further for schemes which will work for a large range of R and consider the Spalding-Patankar (SP) scheme [3] which is very well known in the engineering community. For our simple problem it is

$$\textit{centered difference scheme } (C) \ , \ \textit{if } R \leq 2 \tag{2.11a}$$

$$a \ \frac{f_j - f_{j-1}}{\Delta x} = 0 \qquad (U1S) \ , \ \textit{if } R > 2 \tag{2.11b}$$

That is, when $R > 2$ the flow is regarded as convection-dominated and the diffusion term is dropped. The accuracy of this scheme seems to be questionable. Yet, in practical computation, this scheme has often produced acceptable results. Those involved in practical computation realize that the mesh size is often not as small as one would wish, so the usual order of accuracy for fixed α and sufficiently small Δx may not hold. What needs to be studied is accuracy for finite mesh size, in particular for finite $R = a\,\Delta x/\alpha$. This problem can be very difficult, but for our simple problem we know the exact solution: it is (2.3). Let us first disregard the boundary conditions and simply substitute $f(x) = e^{ax/\alpha}$ into the various difference equations. By definition, the right-hand sides are the discretization errors. We multiply all equations by α/a^2 to scale the coefficients of $e^{ax/\alpha}$ in each term of (2.1) to equal 1. Substitute $e^{ax/\alpha}$ into (2.11b), for example, and obtain

$$\frac{\alpha}{a^2} \ \frac{a}{\Delta x} \ \Big[f(x) - f(x-\Delta x) \Big] = \frac{1}{R} (1-e^{-R}) \ e^{ax/\alpha}$$

So, relative to the solution, as R becomes larger and larger, the discretization error becomes smaller and smaller. Let the coefficient of $e^{ax/\alpha}$ be denoted by E_{U1S}, i.e.

$$E_{U1S} = \frac{1}{R} \ (1 - e^{-R})$$

Similarly,

$$E_c = \frac{1}{2R} \ (e^R - e^{-R}) - \frac{1}{R^2} \ (e^R - 2 + e^{-R})$$

$$E_{u1} = \frac{1}{R} \ (1 - e^{-R}) - \frac{1}{R^2} \ (e^R - 2 + e^{-R})$$

$$E_L = \frac{1}{8R} \ (3e^R + 3 - 7e^{-R} + e^{-2R}) - \frac{1}{R^2} \ (e^R - 2 + e^{-R})$$

$$E_{u2} = \frac{1}{2R} \ (3 - 4e^{-R} + e^{-2R}) - \frac{1}{R^2} \ (e^R - 2 + e^{-R})$$

and if we drop the diffusion part of (2.10) and denote the remaining part by $U2S$, then

$$E_{u2s} = \frac{1}{2R}\left(3 - 4e^{-R} + e^{-2R}\right)$$

The absolute value of these coefficients are plotted against R in figure 3. We note that

$$E_{u1s} \longrightarrow 0 \quad as \quad R \longrightarrow \infty$$

and that

$$E_{u1s} = E_c \quad at \quad R = 2$$

That is, the discretization error for the SP scheme (and also $U2S$) approaches 0 as $R \longrightarrow \infty$, in contrast to the standard schemes; and it is continuous where the scheme changes.

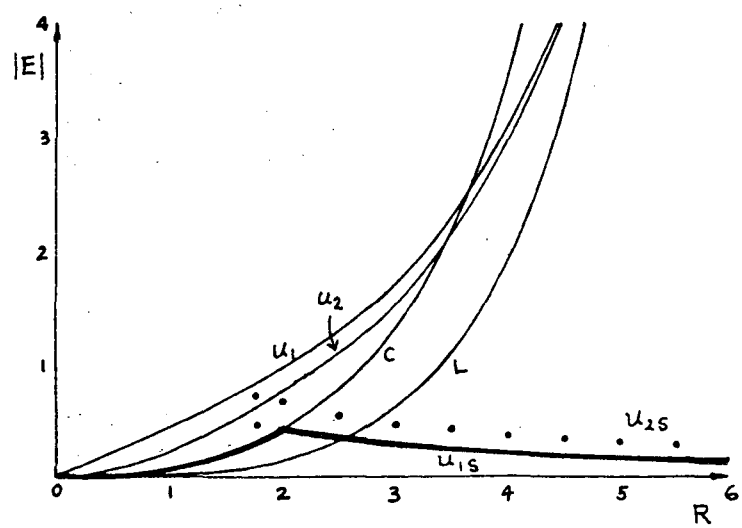

Figure 3: Discretization Error Coefficients vs. Cell Reynolds Number

Let us now take the boundary conditions into consideration and just compare the accuracy of the finite difference solutions for $U1$, SP, and C for fixed Δx and $a/\alpha \longrightarrow \infty$. When $l = 1$, the exact solution of (2.1) and (2.2) is

$$f(x) = \frac{e^{ax/\alpha} - 1}{e^{a/\alpha} - 1} \approx \frac{1}{e^{a/\alpha(1-x)}} = \frac{1}{e^{R(J-j)}}$$

at $x_j = j\Delta x$. The exact solution of $U1$ or C is $f_j = \dfrac{\lambda_2^j - 1}{\lambda_2^J - 1}$

For $U1$ we have from (2.8) $f_j^{u1} = \dfrac{(1+R)^j - 1}{(1+R)^J - 1} \approx \dfrac{1}{(1+R)^{J-j}}$,

and for SP we have $f_j^{SP} = 0$. We see that

$$\epsilon_j^{u1} = f(x_j) - f_j^{u1} \approx \frac{1}{(e^R)^{J-j}} - \frac{1}{(1+R)^{J-j}} \approx \frac{1}{(1+R)^{J-j}}$$

and

$$\epsilon_j^{SP} = f(x_j) - f_j^{SP} \approx \frac{1}{(e^R)^{J-j}}$$

which is smaller than ϵ_j^{u1}. For C we see from (2.6) that the error is large for large R.

The SP scheme is derived from physical considerations; part of the mathematical reason for its success is given here. In the latter part of the next section, extension of its later version to the multi-dimensional case will be commented upon. In general, if used correctly, this scheme has the advantage of being able to calculate large scale phenomena on a rough grid.

However, for many scientific calculations, the boundary layer must be resolved. To do this, either the grid must be sufficiently small near the boundaries or some scheme taking into consideration the nature of the solution near the boundaries must be devised. From what is known of natural convection in enclosures within a certain range of Ra, (see [6] and [7] for example), the flow near the walls has very large gradients. For building energy analysis we will assume that flow at the corners is not important, and will attempt approximation of the solution with exponential functions. In the next section, we discuss the exponential scheme which assumes such an approximation and so will tolerate calculation on a moderate grid even where the gradients are large.

3. The Exponential Scheme

This type of scheme has long been in use; see, for example, [8], [9], and [10], but for the most part only the one-dimensional steady-state case is understood. We will start with this case and then proceed to the multi-dimensional unsteady problems. Consider the equation

$$a \frac{df}{dx} - \alpha \frac{d^2 f}{dx^2} = d \tag{3.1}$$

For the derivation of a discrete equation, a and α are assumed to be constants over the interval $[\,(j-1)\Delta x\ ,\ (j+1)\Delta x\,]$. The exact solution is

$$f(x) = C_1 + C_2\, e^{ax/\alpha} + \frac{d}{a}\, x \tag{3.2}$$

where C_1 and C_2 are determined by f_{j-1} and f_{j+1}, so similar to (2.4):

$$C_1 = \frac{(f_{j-1} - \frac{d}{a} x_{j-1})e^R - (f_{j+1} - \frac{d}{a} x_{j+1})e^{-R}}{e^R - e^{-R}}$$

$$C_2 = \frac{(f_{j+1} - \frac{d}{a} x_{j+1}) - (f_{j-1} - \frac{d}{a} x_{j-1})}{(e^R - e^{-R})\, e^{ax_j/\alpha}}$$

The discrete equation is $f_j = C_1 + C_2\, e^{ax_j/\alpha} + \frac{d}{a} x_j$

Solving for d, we obtain the following form

$$\frac{a}{\Delta x} \frac{-(1 - e^{-R})\, f_{j+1} + (e^R - e^{-R})\, f_j - (e^R - 1)\, f_{j-1}}{e^R - 2 + e^{-R}} = d \ , \quad (3.3)$$

the left-hand side of which approaches the centered difference for the diffusion term as $R \rightarrow 0$ and approaches the upwind difference for the convection term as $R \rightarrow \infty$. Eqn. (3.3) is exact since $f(x)$ is necessarily of form (3.2).

We note the following: first analyzing (3.3) for $d=0$ as in Sec. 2, we get corresponding roots

$$\lambda_1 = 1 \ , \ \lambda_2 = \frac{e^R - 1}{1 - e^{-R}}$$

which are positive for any R and thus no oscillation results. Secondly, for

$$\frac{\partial f}{\partial t} + a \frac{\partial f}{\partial x} - \alpha \frac{\partial^2 f}{\partial x^2} = 0$$

we simply form, for the present, an explicit scheme with the "difference" of (3.3), i.e.,

$$\frac{f_j^{n+1} - f_j^n}{\Delta t} + \frac{a}{\Delta x} \frac{-(1 - e^{-R})\, f_{j+1}^n + (e^R - e^{-R})\, f_j^n - (e^R - 1)\, f_{j-1}^n}{e^R - 2 + e^{-R}} = 0 \quad (3.4)$$

and study its stability. Let

$$A = \frac{R}{e^R - 1} \quad , \quad B = \frac{R\ e^R}{e^R - 1} = R + A \tag{3.5}$$

and $r = a\,\Delta t/\Delta x$, $s = \alpha\Delta t/\Delta x^2$. Assume for the moment that $R > 0$; then (3.4) can be written as

$$f_j^{n+1} = f_j^n + r\ \frac{f_{j+1}^n - (1+e^R)\, f_j^n + e^R\ f_{j-1}^n}{e^R - 1}$$

$$= f_j^n - s\ [(R + A)\,(f_j^n - f_{j-1}^n) - A\,(f_{j+1}^n - f_j^n)\,]$$

$$= f_j^n - s\ R\ (f_j^n - f_{j-1}^n) + s\ A\ (f_{j+1}^n - 2f_j^n + f_{j-1}^n)$$

$$= f_j^n - \frac{sR}{2}\,(f_{j+1}^n - f_{j-1}^n) + (\frac{sR}{2} + sA)\,(f_{j+1}^n - 2f_j^n + f_{j-1}^n)$$

From the stability of the FTSC scheme, we have the stability condition

$$(sR)^2 \leq 2 \qquad \left(\frac{sR}{2} + sA \right) \leq 1$$

The first inequality is but $r^2 \leq r + 2sA$; this is obvious for $r \leq 1$ which we will assume. The second inequality simplifies to the stability condition

$$s\ (A + B) \leq 1 \tag{3.6}$$

We note in passing that this is not a stringent condition since it is dominated by its restriction at $R = 2$ which amounts to

$$r \leq \frac{e^2 - 1}{e^2 + 1} \approx 0.76$$

Stability condition (3.6) holds also for $R < 0$; we will not go into its derivation. Instead, we move on to the multi-dimensional problems.

Often for multi-dimensional and/or unsteady problems, the exponential scheme is obtained by direct extension of (3.3). Take the two-dimensional steady-state equation as an example,

$$a \frac{\partial f}{\partial x} + b \frac{\partial f}{\partial y} - \alpha \left(\frac{\partial^2 f}{\partial x^2} + \frac{\partial^2 f}{\partial y^2} \right) = d \tag{3.7}$$

the discrete equation would be

$$\frac{a}{\Delta x} \frac{-(1 - e^{-R}) f_{j+1,k} + (e^R - e^{-R}) f_{jk} - (e^R - 1) f_{j-1,k}}{e^R - 2 + e^{-R}} + \tag{3.8}$$

$$+ \frac{b}{\Delta y} \frac{-(1 - e^{-S}) f_{j,k+1} + (e^S - e^{-S}) f_{jk} - (e^S - 1) f_{j,k-1}}{e^S - 2 + e^{-S}} = d$$

where R is as defined above and $S = b\Delta y/\alpha$. The first and second term have been regarded respectively as approximations of the x derivative and the y derivative terms.

Here we give a more rigorous derivation. For (3.7) with $d=0$, we try $e^{mx}\ e^{ny}$ as solution and get $am + bn - \alpha(m^2 + n^2) = 0$.
As the task is only to derive a discrete equation, we take just $m = a/\alpha$, $n = 0$; $m = 0$, $n = b/\alpha$; and a linear solution $-bx + ay$; and constant 1, and suppose that the solution is a linear combination of these functions. Or for (3.7), suppose that the solution can be expressed as

$$f(x,y) = C_1(-bx + ay) + C_2 + C_3\, e^{ax/\alpha} + C_4\, e^{by/\alpha}$$

$$+ \frac{d}{q^2}(ax + by) \tag{3.9}$$

where $q^2 = a^2 + b^2$. Let C_1, C_2, C_3, and C_4 be determined by f at the four neighboring points: f_{10}, f_{-10}, f_{01}, and f_{0-1}, (see fig. 4), then

$$\begin{pmatrix} -b\Delta x & 1 & e^R & 1 \\ b\Delta x & 1 & e^{-R} & 1 \\ a\Delta y & 1 & 1 & e^S \\ -a\Delta y & 1 & 1 & e^{-S} \end{pmatrix} \begin{pmatrix} C_1 \\ C_2 \\ C_3 \\ C_4 \end{pmatrix} = \begin{pmatrix} f_{10} & -d & a\Delta x/q^2 \\ f_{-10} & -d & a(-\Delta x)/q^2 \\ f_{01} & -d & b\Delta y/q^2 \\ f_{0-1} & -d & b(-\Delta y)/q^2 \end{pmatrix}$$

or simply $AC = F$; here we have assumed the center point to be at the origin for the sake of convenience. By Cramer's rule $C_i = D_i/D$ where D is the determinant of matrix A and D_i the determinant of the matrix obtained by replacing the ith column of A by F.

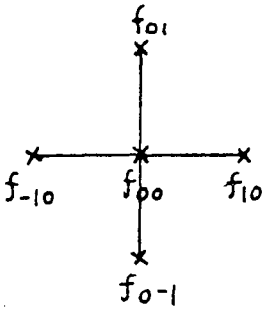

Figure 4: Two-Dimensional Uniform Grid

The D's are given in Table 1a. The discrete equation is just $Df_{00}=D_2+D_3+D_4$ which simplifies to (3.8). This discrete equation is exact if the solution $f(x,y)$ is of form (3.9); see [11] for similar work on compact schemes. In general, the accuracy of the solution will depend on the approximation of the solution by a function of form (3.9). It is important to know the basis and coefficient for approximation since only then can accuracy be analyzed and gradients consistently found.

Table 1a: $c_i = D_i/d$ for Two-Dimensional Uniform Grid

	$F(\Delta x,0)$	$F(-\Delta x,0)$	$F(0,\Delta y)$	$F(0,-\Delta y)$
D_1	$X_b\ Y_c$	$X_f\ Y_c$	$-X_c\ Y_b$	$-X_c\ Y_f$
D_2	$-A(e^{-R}\ Y_a - 2)$ $-B\ \ Y_c$	$A(e^{R}\ Y_a - 2)$ $-B\ \ Y_c$	$-AX_c$ $-B(X_a\ e^{-s} - 2)$	$-AX_c$ $+B(X_a\ e^{s} - 2)$
D_3	AY_2 $+BY_c$	$-AY_2$ $+BY_c$	$-2BY_b$	$-2BY_f$
D_4	$-2AX_b$	$-2AX_f$	AX_c $+BX_2$	AX_c $-BX_2$
D	$AX_c\ Y_2 + BX_2\ Y_c$			

Notation:	$X_b = 1 - e^{-R}$	$X_f = e^{R} - 1$
	$X_c = e^{R} - e^{-R}$	$X_2 = e^{R} - 2 + e^{-R}$
	$X_a = e^{R} + e^{-R}$	$A = a\ \Delta\ y$
	$B = b\ \Delta\ x$	Similarly, for y with S

We proceed now to the three-dimensional unsteady equation

$$\frac{\partial f}{\partial t} + a\,\frac{\partial f}{\partial x} + b\,\frac{\partial f}{\partial y} + c\,\frac{\partial f}{\partial z} - \alpha\left(\frac{\partial^2 f}{\partial x^2} + \frac{\partial^2 f}{\partial y^2} + \frac{\partial^2 f}{\partial z^2}\right) = d \tag{3.10}$$

It turns out that if $f(x,y,z,t)$ can be expressed as

$$\begin{aligned} f(x,y,z,t) &= C_0\,(ax + by + cz - q^2\,t) \\ &+ C_1\,(-bx + ay) + C_2(-cy + bz) + C_3 \\ &+ C_4\,e^{ax/\alpha} + C_5\,e^{by/\alpha} + C_6\,e^{cz/\alpha} \\ &+ \frac{d}{q^2}\,(ax + by + cz) \end{aligned} \tag{3.11}$$

where $q^2 = a^2 + b^2 + c^2$, and if the coefficients are determined by

$$f^{\,0}_{100},\ f^{\,0}_{-100},\ f^{\,0}_{010},\ f^{\,0}_{0-10},\ f^{\,0}_{001},\ f^{\,0}_{00-1},\ \text{and}\ f^{\,1}_{000} - f^{\,0}_{000},$$

where the subscripts denote multiples of Δx, Δy, and Δz in the same order, and the superscripts 0 and 1 denote time level 0 and Δt respectively, then again the resulting discrete equation appears to be the direct extension of the one-dimensional steady-state case. We give a few details. As

$$f(0,0,0,\Delta t) = -C_0\,q^2\,\Delta t + C_3 + C_4 + C_5 + C_6$$

and

$$f(0,0,0,0) = C_3 + C_4 + C_5 + C_6\,,$$

so

$$C_0 = \frac{f^{\,1}_{000} - f^{\,0}_{000}}{-q^2\,\Delta t}$$

is known. The system of linear equations for the coefficients C_1 to C_6 is

$$
\begin{pmatrix}
-b\,\Delta x & 0 & 1 & e^{R} & 1 & 1 \\
b\,\Delta x & 0 & 1 & e^{-R} & 1 & 1 \\
a\,\Delta y & -c\,\Delta y & 1 & 1 & e^{S} & 1 \\
-a\,\Delta y & c\,\Delta y & 1 & 1 & e^{-S} & 1 \\
0 & b\,\Delta z & 1 & 1 & 1 & e^{T} \\
0 & -b\,\Delta z & 1 & 1 & 1 & e^{-T}
\end{pmatrix}
\begin{pmatrix} C_1 \\ C_2 \\ C_3 \\ C_4 \\ C_5 \\ C_6 \end{pmatrix}
=
\begin{pmatrix} F^{0}_{100} \\ F^{0}_{-100} \\ F^{0}_{010} \\ F^{0}_{0-10} \\ F^{0}_{001} \\ F^{0}_{00-1} \end{pmatrix}
$$

or simply $AC = F$, in which

$$F^{0}_{100} = f^{0}_{100} - C_0\, a\,\Delta x - \frac{d}{q^2}\, a\,\Delta x$$

$$F^{0}_{-100} = f^{0}_{-100} - C_0\, a(-\Delta x) - \frac{d}{q^2}\, a(-\Delta x)$$

and similarly for the other F's. As before, $C_i = D_i/D$. The discrete equation is just

$$D\, f^{0}_{000} = D_3 + D_4 + D_5 + D_6$$

which is (replacing 0 0 0 0 with $j\ k\ l\ n$)

$$
\begin{aligned}
&\frac{f^{n+1}_{jkl} - f^{n}_{jkl}}{\Delta t} \qquad\qquad (3.12)\\
&+ \frac{a}{\Delta x}\,\frac{-(1-e^{-R})\, f^{n}_{j+1,\,kl} + (e^{R} - e^{-R})\, f^{n}_{jkl} - (e^{R} - 1)\, f^{n}_{j-1,kl}}{e^{R} - 2 + e^{-R}}\\
&+ \frac{b}{\Delta y}\,\frac{-(1-e^{-S})\, f^{n}_{j,k+1,l} + (e^{S} - e^{-S})\, f^{n}_{jkl} - (e^{S} - 1)\, f^{n}_{j,k-1,l}}{e^{S} - 2 + e^{-S}}\\
&+ \frac{c}{\Delta z}\,\frac{-(1-e^{-T})\, f^{n}_{j,k,l+1} + (e^{T} - e^{-T})\, f^{n}_{jkl} - (e^{T} - 1)\, f^{n}_{j,k,l-1}}{e^{T} - 2 + e^{-T}} = d
\end{aligned}
$$

where R and S are as before and $T = c\,\Delta z/\alpha$. Again, (3.12) is exact for solutions of form (3.11) and in general, the accuracy will depend on the representation

of the solution by the basis.

Nothing has been said about the uniqueness of the given basis. We comment only that since the domain of definition is discrete, some otherwise independent functions may be expressible in terms of the given basis.
For example, let $(e^R, e^{-R}, e^S, e^{-S}, e^T, e^{-T})'$ represent $e^{ax/\alpha}\ e^{by/\alpha}\ e^{cz/\alpha}$ defined at the six points $(\pm\Delta x, 0, 0)$, $(0, \pm\Delta y, 0)$ and $(00, \pm\Delta z)$.
It is just $(\vec{v}_x + \vec{v}_y + \vec{v}_z - \vec{v}_1)$ where the vectors inside the parentheses represent, in order, $e^{ax/\alpha}$, $e^{by/\alpha}$, $e^{cz/\alpha}$, and 1 at the same points.

As to the completeness of the given basis on the discrete domain, we note only that the schemes are derived for $a \neq 0$, $b \neq 0$, $c \neq 0$. For $a = 0$, for instance, the a term in (3.8) and (3.12) becomes simply the second order centered difference approximation to $\alpha \dfrac{d^2 f}{d\ x^2}$, which is correct.

The exponential function was also used for the later *SP* scheme [3]. The idea is as follows: consider (2.1) and (2.3), assume a and α to be constant in the interval $[j\Delta x\ ,\ (j+1)\ \Delta x]$, and determine C_1 and C_2 by f_j and f_{j+1}. Then the flux in this interval, especially at the middle of the interval, is

$$(\ flux\ )_{j+\frac{1}{2}} = (af\ - \alpha \frac{df}{dx})_{j+\frac{1}{2}} = a\ C_1 = a\ \frac{e^R\ f_j - f_{j+1}}{e^R - 1} \tag{3.13}$$

from (2.4). The discrete equation at j is formed as $(\ flux\ )_{j+\frac{1}{2}} - (\ flux\ )_{j-\frac{1}{2}} = 0$ which turns out to be just (3.3) with $d = 0$. *SP* schemes for more complicated cases are formed via control volume but with flux still in the form (3.13). This turns out to be fine for a uniform grid. As a matter of fact, they are identical with the exponential schemes derived above. But for a nonuniform grid, with the exception of the simplest case above, the consistency conditions are not satisfied. To emphasize this point, we will just take the simplest case of equation (3.1) with grid as shown in figure 5. The *SP* scheme is

$$(\ flux\ )_{j+\frac{1}{2}} - (\ flux\ )_{j-\frac{1}{2}} = dh$$

where h is the length of the control "volume", which is equal to $3\Delta x/4$. For simplicity, we consider only the limit as $R \longrightarrow \infty$, in which case $(\ flux\ )_{j+\frac{1}{2}}$ reduces to af_j, so

$$\frac{4}{3\Delta x}\ (af_j - af_{j-1}) = d$$

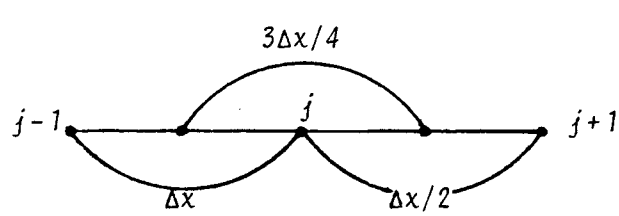

Figure 5: One-Dimensional Non-Uniform Grid

which, of course, is not consistent with (3.1). However, if the grid size varies gradually, then the *SP* scheme is not far from the truth, in practical computation perhaps not further from the truth than other assumptions, for example constancy of the coefficients.

It should be noted that, in general, (3.13) is not the real flux. Even with just a non-homogeneous term in the one-dimensional steady-state case, the flux becomes

$$(flux)_{j+½} = (af - \alpha \frac{df}{dx})_{j+½} = aC_1 + dx_{j+½} - \alpha \frac{d}{a}$$

where

$$C_1 = \frac{e^R (f_j - \frac{d}{a} x_j) - (f_{j+1} - \frac{d}{a} x_{j+1})}{e^R - 1}$$

which is not (3.13). However, since on a uniform grid the *SP* schemes are identical with the exponential schemes, we will borrow the idea of flux in the form of (3.13) and put the exponential schemes into conservation form, which facilitates computation. We will call (3.13) the mathematical flux. For example, (3.8) can be written in the form

$$\frac{1}{\Delta x} (F^x_{j+½,k} - F^x_{j-½,k}) + \frac{1}{\Delta y} (F^y_{j,k+½} - F^y_{j,k-½}) = d$$

where

$$F^x_{j+½,k} = a \frac{e^R f_{jk} - f_{j+1,k}}{e^R - 1}$$

$$F^y_{j,k+½} = b \frac{e^S f_{jk} - f_{j,k+1}}{e^S - 1}$$

are the mathematical fluxes.

Though our computation of the two-dimensional model problem of natural convection will be done on a uniform grid (see fig. 4); at the boundary it will involve a non-uniform grid as shown in fig. 6 for the right boundary, with boundary point b at distance $\Delta x/2$ to the right of the center point. We derive the discrete equation as before, except the coefficients in (3.9) are determined by f_b, f_{-10}, f_{01}, and f_{0-1}. The corresponding D's are given in Table 1b and the discrete equation is

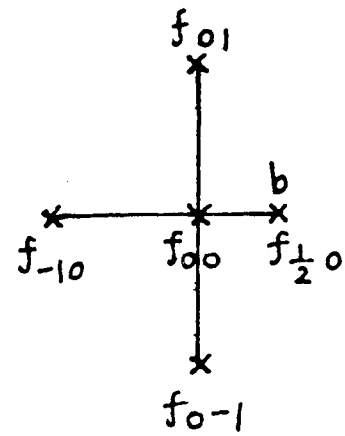

Figure 6:
Two-Dimensional Non-Uniform Grid

$$\frac{a}{\Delta x}\;\frac{-(1-e^{-R})\,f_b + (e^{R/2}-e^{-R})\,f_{00} - (e^{R/2}-1)\,f_{-10}}{e^{R/2}-3/2+e^{-R/2}}$$

$$+\;\frac{b}{\Delta y}\;\frac{-(1-e^{-S})\,f_{01} + (e^{S}-e^{-S})\,f_{00} - (e^{S}-1)\,f_{0,-1}}{e^{S}-2-e^{-S}} = d \tag{3.14}$$

This can be written as

$$\frac{1}{\Delta x}\left(F_b^x - F^x_{-\frac{1}{2},0}\right) + \frac{1}{\Delta y}\left(F^y_{0,\frac{1}{2}} - F^y_{0,-\frac{1}{2}}\right) = d \tag{3.15}$$

where $F^x_{-\frac{1}{2},0}$, $F^y_{0,\frac{1}{2}}$, and $F^y_{0,-\frac{1}{2}}$, are given by (3.13) but F_b^x is defined as the boundary mathematical flux such that (3.14) is put into form (3.15). Then

$$F_b^x = a\,(k_b\,f_b + k_0\,f_{00} + k_{-1}\,f_{-10})$$

where k_b, k_0, k_{-1} and their limits as $R \to 0$ are such that

$$R\;k_b = -\frac{R\,(e^{-R}+e^{-R/2})}{(2-e^{-R}-e^{-R/2})/2} \to -\frac{8}{3}$$

$$R\;k_0 = \frac{R\,(e^{-R}+e^{-R/2}+1)}{(2-e^{-R}-e^{-R/2})/2} - \frac{R}{e^{R}-1} \to -3$$

$$R\;k_{-1} = -\frac{R}{(2-e^{-R}-e^{-R/2})/2} + R\,\frac{e^{R}}{e^{R}-1} \to -\frac{1}{3}, \quad as\ R \to 0$$

So, at the boundary where $u = v = 0$, we have

$$F_b = \frac{\alpha}{\Delta x} \left(-\frac{8}{3} f_b + 3 f_{00} - \frac{1}{3} f_{-1,0} \right) \tag{3.16}$$

This is a second order approximation of $(-\alpha \, \partial f / \partial x)_b$, which is the flux at the boundary. That is, the defined boundary mathematical flux in this case turns out to be the real flux.

Table 1b: $c_i = D_i / d$ for Two-Dimensional Non-Uniform Grid (Fig. 6 with $\theta = \frac{1}{2}$)

	$F(\frac{\Delta x}{2},0)$	$F(-\Delta x,0)$	$F(0,\Delta y)$	$F(0,\Delta y)$
D_1	$X_b \; Y_c$	$X_f' \; Y_c$	$-X_c' \; Y_b$	$-X_c' \; Y_f$
D_2	$-A(e^{-R} \; Y_a - 2)$ $-B \; Y_c$	$A(e^{\theta R} \; Y_a - 2)$ $-\theta B \; Y_c$	$-AX_c'$ $-B(X_a' \; e^{-s} - 1 - \theta)$	$-AX_c'$ $+B(X_a' \; e^{-s} - 1 - \theta)$
D_3	AY_2 $+BY_c$	$-AY_2$ $+\theta BY_c$	$-(1+\theta) \; BY_b$	$-(1+\theta) \; BY_f$
D_4	$-2AX_b$	$-2AX_f'$	AX_c' $+BX_2'$	AX_c' $-BX_2'$
D	$AX_c' \; Y_2 + BX_2' \; Y_c$			

Notation:	$X_f' = e^{\theta R} - 1$	$X_c' = e^{\theta R} - e^{-R}$
	$X_2' = e^{\theta R} - (1+\theta) + \theta e^{-R}$	$X_a' = e^{\theta R} + \theta e^{-R}$

4. Numerical Solution of the Boussinesq Equations

The explicit exponential scheme will be adapted to the computation of natural convection flow. Our method will be based on the well-known MAC (Marker and Cell) finite difference method of the incompressible Navier-Stokes equations in primitive variables given by Harlow and Welch [4]. Its main features are:

(1) The finite difference scheme is FTCS (forward time centered space), which can easily be changed to allow better stability conditions, (see [12]).

(2) The computation is done on a staggered mesh as shown in fig. 7.

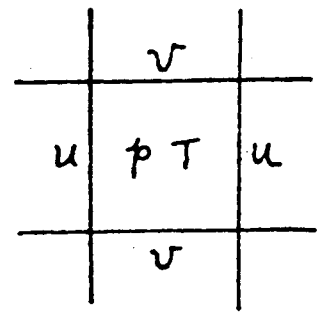

Figure 7: Staggered Mesh

(3) The Poisson difference equation for pressure is obtained by differencing the x and y momentum difference equations, with respect to x and y respectively, and then adding them together. In the resulting $(D^{n+1} - D^n)/\Delta t$, D^{n+1} is set to zero to ensure the constraint (1.1).

(4) The D^n in this term, as well as $\nabla^2 D^n$ from the other terms, is kept in the difference equation so that the errors from the iterative solution of the Poisson difference equation do not accumulate.

(5) The boundary conditions for the Poisson equation are derived naturally from the momentum equations, from which the Poisson equation itself is derived. According to Easton [13], finite difference approximations need not be formed for these boundary conditions; all that is necessary is to cancel its corresponding difference parts in the Poisson difference equation. So $\Delta\phi/\Delta n$ on the boundary does not appear in the Poisson difference equation. The procedure is greatly simplified.

The author believes that the last two features are important in keeping the difference forms of the original equations and the Poisson equation equivalent in the interior and on the boundary. As we all know, equivalence in differential form is not always carried over to its difference form. Unless the non-equivalence can be used to one's advantage, for example in shock calculation to ensure entropy increase, it is best to keep the equivalence in difference forms, so that the inconsistencies do not work against the purpose.

For our model problem, we will use the staggered mesh as shown in fig. 7, but now the scaled pressure ϕ and the scaled temperature θ will be at the center of the mesh. The Boussinesq equations (1.1) to (1.4) are cast into the following difference form

$$\frac{\delta_x\, u}{\Delta x} + \frac{\delta_y\, v}{\Delta y} = 0 \tag{4.1}$$

$$\frac{u^{n+1} - u^n}{\Delta t} + \frac{\delta_x\, F_x}{\Delta x} + \frac{\delta_y\, F_y}{\Delta y} + \frac{\delta_x\, \phi}{\Delta x} = 0 \tag{4.2}$$

$$\frac{v^{n+1} - v^n}{\Delta t} + \frac{\delta_x\ G_x}{\Delta x} + \frac{\delta_y\ G_y}{\Delta y} + \frac{\delta_y\ \phi}{\Delta y} = Gr\ \theta \tag{4.3}$$

$$\frac{\theta^{n+1} - \theta^n}{\Delta t} + \frac{\delta_x\ H_x}{\Delta x} + \frac{\delta_y\ H_y}{\Delta y} = 0 \tag{4.4}$$

where δ_x and δ_y are respectively the centered x and y differences. F_x, F_y, G_x, G_y, H_x, and H_y, are the x and y (as the subscripts indicate) mathematical fluxes as defined in Sec. 3, i.e. for the x case,

$$(math\ flux)_{j+\frac{1}{2},k} = \frac{\alpha}{\Delta x}\left(B\ f_{jk} - A\ f_{j+1,k}\right) \tag{4.5}$$

where A and B are defined as (3.5). For the y case, $j,k,\Delta x$ and R become $k,j,\Delta y$ and S respectively. For (4.2), f is u, for (4.3) f is v, and α=1. For (4.4), f is θ and $\alpha=1/Pr$. At the boundary, these fluxes are

$$(flux)_{j\mp\frac{1}{2},k} = \frac{\alpha}{\Delta x}\left(\pm\frac{8}{3}f_{j\mp\frac{1}{2},k} \mp 3\ f_{jk} \pm \frac{1}{3}f_{j\pm1,k}\right) \tag{4.6}$$

as (3.16); similarly for k.

That is, the exponential scheme is used for the equations with convection and dissipation (or diffusion) terms. As is usually done with exponential schemes for non-linear equations, the unknowns in the coefficients are assumed to be piecewise constants, but in the partial differentials they are assumed to be locally approximated by exponential functions. This discrepancy may not be too serious in our model problem since u does not vary drastically in the x direction and v does not vary drastically in the y direction. Centered difference is used for ϕ since it is well behaved.

The features (3) and (5) of the MAC method are maintained in our method so that the Poisson difference equation

$$\frac{\delta_x}{\Delta x}\left(\frac{\delta_x\phi}{\Delta x}\right) + \frac{\delta_y}{\Delta y}\left(\frac{\delta_y\phi}{\Delta y}\right) = \tag{4.7}$$

$$-\left(-\frac{D^n}{\Delta t} + \frac{\delta_x}{\Delta x}\left(\frac{\delta_x F_x}{\Delta x}\right) + \frac{\delta_x}{\Delta x}\left(\frac{\delta_y F_y}{\Delta y}\right)\right.$$

$$\left. + \frac{\delta_y}{\Delta y}\left(\frac{\delta_x G_x}{\Delta x}\right) + \frac{\delta_y}{\Delta y}\left(\frac{\delta_y G_y}{\Delta y}\right) - Gr\ \frac{\delta_y\ \theta}{\Delta y}\right)$$

and the corresponding boundary conditions result. On the left boundary, for example, the corresponding $\delta_x \phi/\Delta x$, $\delta_x F_x/\Delta x$, and $\delta_y F_y/\Delta y$, cancel out, u being zero. Hence, (4.7) is equivalent to (4.1), (4.2), (4.3) on the boundary as well as in the interior of the computational region. And we will see in the numerical tests that the iterative errors of (4.7) do not accumulate as n advances.

We state finally the computational steps:

(1) Given u^n, v^n, and θ^n, calculate F_x^n, F_y^n, G_x^n, G_y^n, H_x^n, and H_y^n, with (4.5) and (4.6); from (1.6) we have $H_y=0$ on the top and bottom boundaries.

(2) Calculate the right-hand side of (4.7) and solve (4.7) for ϕ, with $D^{n+1}=0$, i.e. (4.1), enforced.

(3) Compute u^{n+1} from (4.2).

(4) Compute v^{n+1} from (4.3).

(5) Compute θ^{n+1} from (4.4).

Test calculations for various aspect ratios H/L, Prandtl numbers, and Rayleigh numbers are being carried out; the results versus experimental results will be reported elsewhere. Here we present only the test calculations for aspect ratio 1, $Pr=0.71$ (air), $Ra=10^6$ and 10^7. The initial conditions are $u=v=0$ and $\theta=\theta_c=0$. For the solution of the Poisson difference equation, the point Gauss-Seidel method was used for its simplicity. For the mathematical fluxes the Spalding-Patankar approximation for A and B [3] were used to avoid calling the exponential function with excessive frequency. The stability condition was taken to be

$$s \leq \frac{\gamma}{max\left[\, max_{jk}\,(A_x + B_x)\,,\; max_{jk}\,(A_y + B_y)\,\right]}$$

where $\gamma \leq 0.5$, and where A and B denote coefficients from the temperature field and the subscripts denote the directions of the fluxes. For these preliminary calculations, no attempt was made to study stability any further, either for two dimensions or for non-homogeneous terms.

For $Ra = 10^6$, the estimated boundary layer thickness $b=0.032$, a 36x36 grid was used, i.e. $\Delta x=\Delta y=0.0278$, giving one mesh point at $<0.9\ b$ in the boundary layer. For $Ra = 10^7$, the estimated boundary layer thickness $b=0.018$, a 64x64 grid was used, i.e. $\Delta x=\Delta y=0.015625$ giving also one mesh point at $<0.9b$ in the boundary layer.

Before presenting the computational results, we note that the iterative errors of ϕ indeed did not accumulate. For example for the $Ra = 10^6$ case, the error tolerance for ϕ, $\max_{jk} |\phi_{jk}^{\mu+1}-\phi_{jk}^{\mu}|/\max_{jk} |\phi_{jk}^{\mu}|$ was 0.001; therefore, (4.7) or (4.1) was not satisfied exactly.
In the beginning, $d=max|D_{jk}|/(max_{jk}|u_{jk}|+max_{jk}|v_{jk}|)=0.9\times10^{-1}$, but as the computation proceeded it decreased and upon convergence to steady state, $d=0.2\times10^{-3}$.

We compare our numerical results with those of the DeVahl Davis benchmark [6] for $Ra=10^6$ and the accurately computed results of LeQuere [7] for $Ra=10^7$. Table 2 gives $umax$ on the vertical mid-plane and $vmax$ on the horizontal mid-plane and their respective positions; for the sake of comparison these are found as [6]. The average Nusselt numbers on the left wall are also given, which should equal those on any vertical plane upon steady state. Our Nu, u, and v are multiplied by Pr to have the same dimensionality. We note especially that with one mesh point located at $<0.9b$ in the boundary layer, the error of the average Nusselt number at the wall is less than 4% in both cases.

Table 2

	Ra	$umax$	z	$vmax$	x	$(Nu)h$	$(Nu)c$
DeVahl Davis[6]	10^6	64.83	.850	220.56	.0375	8.835	
This work	10^6	65.37	.846	217.38	.0356	9.139	9.121
LeQuere[7]	10^7	148.8	.879	699.3	.0213	16.52	
This work	10^7	141.9	.889	691.3	.0201	17.14	17.139

We look now at the general flow pattern. The isotherms and the streamlines from our numerical results are given in figs. 8 and 9. They agree in general with the corresponding figures in [6] and [7]. However, for $Ra=10^7$, the flow pattern near the top and bottom walls remains smooth, whereas it becomes somewhat wavy in [7]. For flow patterns and Nusselt numbers in building environments with a wide range of Ra, one can consult Gadgil [14].

5. Conclusion

In this paper, an approximating basis has been found for the multidimensional unsteady exponential scheme. A boundary exponential scheme has also been derived. These schemes in conservation form are adapted to the Boussinesq equations, retaining the equivalence of the momentum equations with the Poisson equation; numerical tests show that indeed the iterative errors do not accumulate. The exponential scheme has been tested especially for natural convection flow in a cavity with only one mesh point in the boundary layer. Numerical tests show that for $Ra=10^6$ and $Ra=10^7$ the accuracy in the average Nusselt numbers suffice for some engineering purposes. Improvements are planned to decrease the computing time, since no such efforts have been made in this work. For high Ra, the finer features of the flow in the interior of the region may be lost. Hence, improvement of the quality of the numerical solution is also necessary. Efforts will be made in two different directions: use of a global variable grid with a local uniform grid according to Berger and Oliger [15], and consideration of singular perturbation problems in the development of numerical methods. For $Ra = 10^9 - 10^{12}$, typical in building energy analysis, mathematical formulation with turbulence will be investigated.

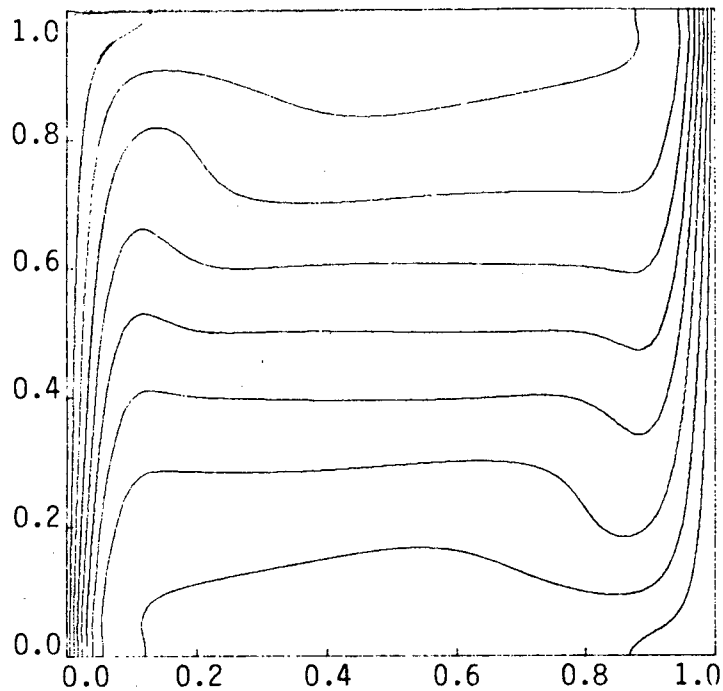

Isotherms. Isovalues are 0.1 (0.1) 0.9

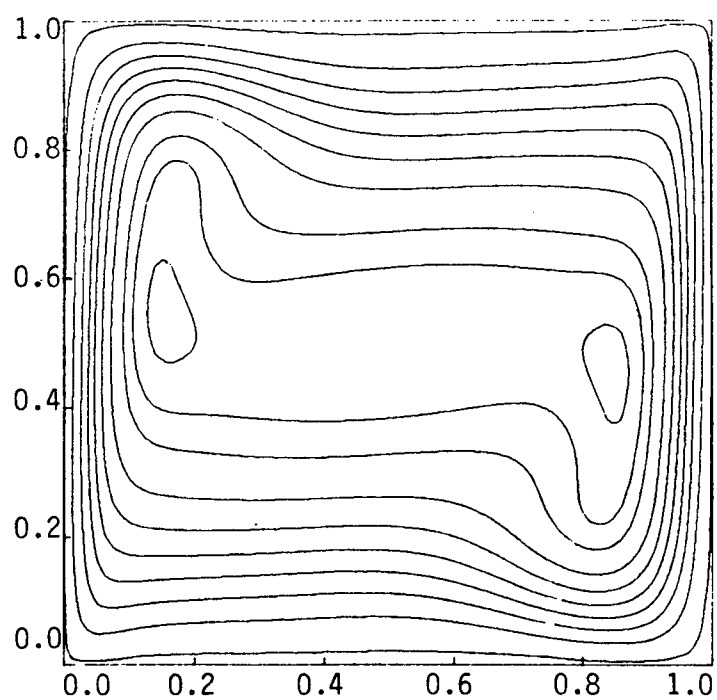

Streamfunction. Isovalues are 0.213 2.144 (2.144) 15.052 16.124 16.983

Figure 8: Calculated streamfunction and isotherms for $Ra=10^6$ with a 36x36 grid

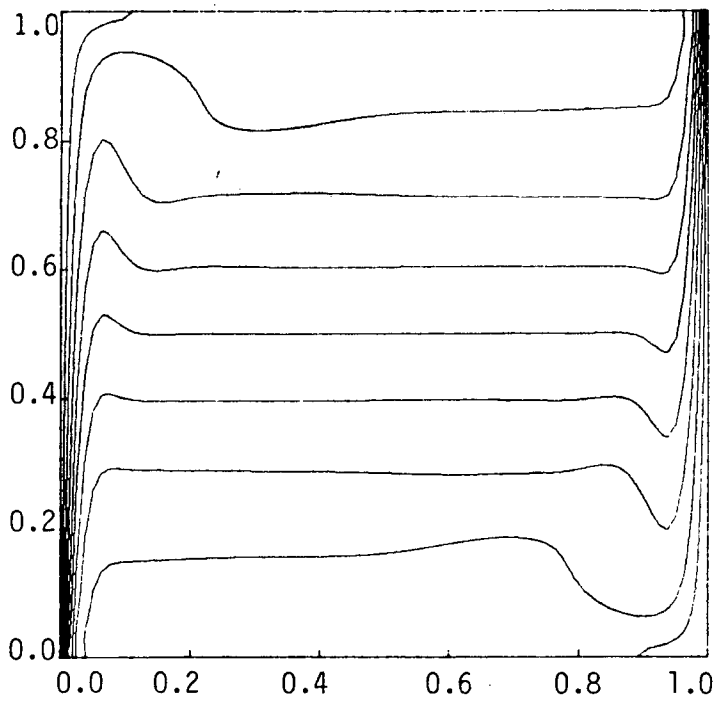

Isotherms. Isovalues are 0.1 (0.1) 0.9

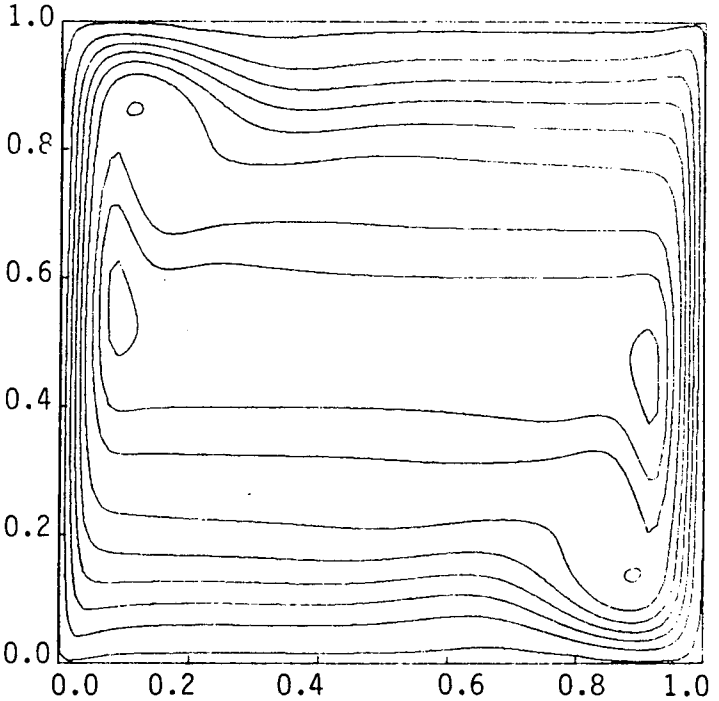

Streamfunction. Isovalues are 0.44 4.41 (4.41) 26.44 28.64 30.40

Figure 9: Calculated streamfunction and isotherms for $Ra=10^7$ with a 64x64 grid

6. Acknowledgment

This work is part of a research effort toward development of the next generation of building energy simulation programs — a cooperative effort between the Lawrence Berkeley Laboratory (University of California) and the Computing Center of the Chinese Academy of Sciences. The author wishes to thank Frederick Winkelmann, James J. Hirsch, Arthur H. Rosenfeld, and and the members of LBL's Simulation Research Group for their generous encouragement, patience, and helpful suggestions.

REFERENCES

1. Bauman, F. et.al., **Convection Heat Transfer in Buildings: Recent Research Results,** Lawrence Berkeley Laboratory, Report No. LBL-13883 Rev., 1982. ASHRAE Transactions 88 (1983).
2. DeVahl Davis, G. and Jones, I. P., **Natural Convection in a Square Cavity: A Comparison Exercise,** Int. J. Num. Meth. in Fluids 3 (1983), 227.
3. Patankar, S. V., **Numerical Heat Transfer and Fluid Flow,** Hemisphere Pub. Corp., 1980.
4. Harlow, F. H. and Welch, J. E. **Numerical Calculation of Time-Dependent Viscous Incompressible Flow of Fluid with Free Surface,** Physics of Fluids 8 (1965), 2182.
5. Leonard, B. P., **A Stable and Accurate Convective Modelling Procedure Based on Quadratic Upstream Interpolation,** Comput. Meth. Appl. Mech. Eng. 19 (1976), 59.
6. DeVahl Davis, G., **Natural Convection of Air in a Square Cavity: A Benchmark Numerical Solution,** Int. J. Num. Meth. in Fluids 3 (1983), 249.
7. LeQuere, P. and DeRoquefort, T.A., **Computation of Natural Convection in Two-Dimensional Cavities with Chebyshev Polynomials,** J. Comput. Phys. 57 (1985), 210.
8. Allen, D. N. de G. and Southwell, R. V., **Relaxation Methods Applied to Determine the Motion, in Two Dimensions, of a Viscous Fluid Past a Cylinder,** Quart. J. Mech. Appl. Math. 8 (1955), 129.
9. Dennis, S. C. R. and Hudson, J. D. **Further Accurate Representation of Partial Differential Equations by Finite Difference Methods,** J. Inst. Math. Appl. 26 (1980), 369.
10. Roach, R. L., **A Consistent Finite Difference Derivation for the Navier-Stokes Equations,** AIAA Paper 82-0102, 1982.
11. Giles, M. B. and Rose, M. E., **A Numerical Study of the Steady Scalar Convective Diffusion Equation for Small Viscosity,** J. Comput. Phys. 56 (1984), 513.

12. Sheng, J. X. and Huang, L. C., **Computation of Natural Convection Flow,** Technical Report, 1984, to be presented at the Third Chinese Conference of Computational Fluid Dynamics.

13. Easton, C. P., **Homogeneous Boundary Conditions for Pressure in the MAC Method,** J. Comput. Phys. 9 (1972), 375.

14. Gadgil, A., **On Convective Heat Transfer in Building Energy Analysis,** Lawrence Berkeley Laboratory, Report No. LBL-10900 (1980).

15. Berger, M. and Oliger, J., **Adaptive Mesh Refinement for Hyperbolic Partial Differential Equations,** J. Comput. Phys. 53 (1984), 484.

LAWRENCE BERKELEY LABORATORY
TECHNICAL INFORMATION DEPARTMENT
UNIVERSITY OF CALIFORNIA
BERKELEY, CALIFORNIA 94720